Research Article

The Second-Order Born Approximation in Diffuse Optical Tomography

Kiwoon Kwon

Department of Mathematics, Dongguk University, Seoul 100715, Republic of Korea

Correspondence should be addressed to Kiwoon Kwon, kwkwon@dongguk.edu

Diffuse optical tomography is used to find the optical parameters of a turbid medium with infrared red light. The problem is mathematically formulated as a nonlinear problem to find the solution for the diffusion operator mapping the optical coefficients to the photon density distribution on the boundary of the region of interest, which is also represented by the Born expansion with respect to the unperturbed photon densities and perturbed optical coefficients. We suggest a new method of finding the solution by using the second-order Born approximation of the operator. The error analysis for the suggested method based on the second-order Born approximation is presented and compared with the conventional linearized method based on the first-order Born approximation. The suggested method has better convergence order than the linearized method, and this is verified in the numerical implementation.

1. Introduction

Diffuse optical tomography involves the reconstruction of the spatially varying optical properties of a turbid medium. It is usually formulated as inverse problem with respect to the forward problem describing photon propagation in the tissue for given optical coefficients [1].

The forward model is described by the photon diffusion equation with the Robin boundary condition. In the frequency domain, it is given by

$$-\nabla \cdot (\kappa \nabla \Phi) + \left(\mu_a + \frac{i\omega}{c}\right)\Phi = q \quad \text{in } \Omega,$$

$$\Phi + 2a\nu \cdot (\kappa \nabla \Phi) = 0 \quad \text{on } \partial\Omega, \tag{1.1}$$

where Ω is a Lipschitz domain in $\mathbb{R}^n$, $n = 2, 3, \dots$, $\partial\Omega$ is its boundary, ν is the unit outward normal vector on the boundary, Φ is the photon density, q is a source term, a is a refraction

parameter, and μ_a, μ'_s, and $\kappa = 1/3(\mu_a + \mu'_s)$ are the absorption, reduced scattering, and diffusion coefficients, respectively. Assume that a is a constant and κ, μ_a, μ'_s are scalar functions satisfying

$$0 < L \leq \kappa, \mu_a, \mu'_s, a \leq U \tag{1.2}$$

for positive constants L and U. The unique determination of the optical coefficients is studied in electrical impedance tomography problem [2–5] and some elliptic problem [6], which is applicable to diffuse optical tomography problem also. Let us denote $x = (\mu_a, \kappa)$ and $\Phi = \Phi(x)$ to emphasize the dependence of Φ on the optical coefficient x.

Assuming we know some a priori information x_0 about the structural optical coefficients x and the perturbation of the optical coefficients $\delta x = x - x_0$, the diffuse optical tomography problem is to find the perturbation of the optical coefficients δx from the difference $\Phi(x + \delta x) - \Phi(x)$ between the perturbed and unperturbed photon density distribution on the boundary $\partial \Omega$. The relation between δx and $\Phi(x + \delta x) - \Phi(x)$ is given by the following Born expansion [7, 8]:

$$\Phi(x + \delta x) - \Phi(x) = \mathcal{R}^1(x, \delta x) + \mathcal{R}^2\left(x, (\delta x)^2\right) + \cdots, \tag{1.3}$$

where

$$\mathcal{R}^0(x) = \Phi(x),$$

$$\mathcal{R}^i\left((\delta x)^i\right) = \mathcal{R}\left(\delta x, \mathcal{R}^{i-1}\left((\delta x)^{i-1}, f\right)\right), \quad i = 1, 2, \ldots,$$

$$\mathcal{R}(\delta x, f) = \mathcal{R}_{\mu_a}(\delta x, f) + \mathcal{R}_\kappa(\delta x, f), \tag{1.4}$$

$$\mathcal{R}_{\mu_a}(\delta x, f) = \int_\Omega \delta\mu_a(\eta) R(\cdot, \eta) f(\eta) d\eta,$$

$$\mathcal{R}_\kappa(\delta x, f) = \int_\Omega \delta\kappa(\eta) \nabla R(\cdot, \eta) \cdot \nabla f(\eta) d\eta,$$

and $R(\cdot, \eta)$ is the Robin function for a source at η, which is the solution of (1.1) for the optical coefficient x when q is the Dirac delta function. By definition of (1.4), the operator $\mathcal{R}$ and $\mathcal{R}^1$ are different in the following sense:

$$\mathcal{R}^1(\delta x) = \mathcal{R}\left(\delta x, \mathcal{R}^0\right) = \mathcal{R}(\delta x, \Phi). \tag{1.5}$$

Let the perturbation of the coefficients be $\delta x^\dagger$ when we neglect second-order terms and higher in the Born expansion (1.3). We can then formulate the linearized diffuse optical tomography problem to find $\delta x^\dagger$ from the following equation, which is the first-order Born approximation:

$$\mathcal{R}^1\left(\delta x^\dagger\right) = \Phi(x + \delta x) - \Phi(x). \tag{1.6}$$

This linearized diffuse optical tomography problem is simple to implement and widely used [9, 10].

In this paper, a new method, which is more accurate than the linearized method, will be suggested (1.6), which is based on the second-order Born approximation. And the method is faster than the full nonlinear method [11]. Let the solution of the proposed method in this paper be δx^B, and let δx be sufficiently small. Then, the error for the linearized solution $\delta x^\dagger$ and the proposed solution δx^B is given by

$$\left\| \delta x^\dagger - \delta x \right\|_{\mathcal{A}} \le C^\dagger \|\delta x\|_{\mathcal{A}}^2, \tag{1.7a}$$

$$\left\| \delta x^B - \delta x \right\|_{\mathcal{A}} \le C^B \|\delta x\|_{\mathcal{A}}^3, \tag{1.7b}$$

where $\mathcal{A} = L^\infty(\Omega) \times L^\infty(\Omega)$ and $C^\dagger$ and C^B are constants which are independent of δx. Hence, the error of the proposed solution x^B in (1.7b) is of the order $O(\|\delta x\|_{\mathcal{A}}^3)$, which is higher than the order of the error of the linearized solution $x^\dagger$, $O(\|\delta x\|_{\mathcal{A}}^2)$.

The detailed statement with proof will be proved in Section 2. Numerical algorithm involving the detailed computation of the second-order term is given in Section 3. Numerical implementation of the proposed method and the linearized method is given in Section 4, and the conclusion of the paper is given in Section 5.

2. Error Analysis

Instead of solving linearized solution $\delta x^\dagger$ in (1.6), we suggest the second order solution δx^B satisfying

$$\mathcal{R}^1\left(\delta x^B\right) = (\Phi(x + \delta x) - \Phi(x)) - \mathcal{R}^2\left(\delta x^\dagger\right)^2, \tag{2.1}$$

or equivalently,

$$\mathcal{R}^1\left(\delta x^B - \delta x^\dagger\right) = -\mathcal{R}^2\left(\delta x^\dagger\right)^2. \tag{2.2}$$

In this section, we analyze the error for the linearized solution $\delta x^\dagger$ and the suggested solution δx^B.

Let $\mathcal{B} = H^1(\Omega)$; then, the operator $\mathcal{R}$ and $\mathcal{R}^i$, $i = 1, 2, \ldots$, are considered to be the operators from $\mathcal{A} \times \mathcal{B} \to \mathcal{B}$ and $\mathcal{A}^i(= \overbrace{\mathcal{A} \times \cdots \times \mathcal{A}}^{i\,\text{times}}) \to \mathcal{B}$, respectively, by the definition given in (1.4). For the detailed explanation about the definitions of higher-order Fréchet derivative in diffuse optical tomography and its relation to the Born expansion, see [7].

Proposition 2.1. *Let Φ be the solution of* (1.1) *for the given optical coefficients μ_a, κ, source q, and modulating frequency ω. Then one gets the following relation between the operators between $\mathcal{R}$ and $\mathcal{R}^i$, $i = 1, 2, \ldots$:*

$$\left\| \mathcal{R}^i \right\|_{\mathcal{A}^i \to B} \le \|\mathcal{R}\|_{\mathcal{A} \times \mathcal{B} \to B}^i \|\Phi\|_{\mathcal{B}} \tag{2.3}$$

for $i = 1, 2, \ldots$.

Proof. By the induction argument on $i = 1, 2, \ldots$ and using (1.5), we get the following inequality:

$$\left\| \mathcal{R}^1 \right\|_{\mathcal{A} \to \mathcal{B}} \leq \|\mathcal{R}\|_{\mathcal{A} \times \mathcal{B} \to \mathcal{B}} \|\Phi\|_{\mathcal{B}}, \tag{2.4}$$

which is (2.3) for $i = 1$. Suppose that (2.3) holds for $i = 1, 2, \ldots, I - 1$. Then we obtain

$$\begin{aligned}
\left\| \mathcal{R}^I (\delta x)^I \right\|_{\mathcal{B}} &\leq \|\mathcal{R}\|_{\mathcal{A} \times \mathcal{B} \to \mathcal{B}} \|\delta x\|_{\mathcal{A}} \left\| \mathcal{R}^{I-1} (\delta x)^{I-1} \right\|_{\mathcal{B}} \\
&\leq \|\mathcal{R}\|_{\mathcal{A} \times \mathcal{B} \to \mathcal{B}} \|\delta x\|_{\mathcal{A}} \left\| \mathcal{R}^{I-1} \right\|_{\mathcal{A}^{I-1}} \|\delta x\|_{\mathcal{A}}^{I-1} \\
&\leq \|\mathcal{R}\|_{\mathcal{A} \times \mathcal{B} \to \mathcal{B}}^{I} \|\delta x\|_{\mathcal{A}}^{I} \|\Phi\|_{\mathcal{B}}.
\end{aligned} \tag{2.5}$$

Using (2.5) and the definition of the operator norm $\| \cdot \|_{\mathcal{A}^I \to \mathcal{B}}$, we obtain (2.3) for $i = I$. Therefore, by the induction argument, we have proved (2.3) for $i = 1, 2, \ldots$. $\qquad \square$

By [7], $\|\mathcal{R}\|_{\mathcal{A} \times \mathcal{B} \to \mathcal{B}}$ is bounded, and thus $\|\mathcal{R}^i\|_{\mathcal{A}^i \to \mathcal{B}}$, $i = 1, 2, \ldots$, are also bounded by Proposition 2.1. Let us assume that there exists a bounded operator $(\mathcal{R}^1)^\dagger$ from $\mathcal{B}$ to $\mathcal{A}$ such that $(\mathcal{R}^1)^\dagger (\mathcal{R}^1) = id_{\mathcal{A}}$. $(\mathcal{R}^1)^\dagger$ is usually called the left inverse of $\mathcal{R}^1$. Let us denote

$$\begin{aligned}
\|\delta x\| &:= \|\delta x\|_{\mathcal{A}}, \\
\|\Phi(x)\| &:= \|\Phi(x)\|_{\mathcal{B}}, \\
\|\mathcal{R}\| &:= \|\mathcal{R}\|_{\mathcal{A} \times \mathcal{B} \to \mathcal{B}}, \\
\left\| \mathcal{R}^i \right\| &:= \left\| \mathcal{R}^i \right\|_{\mathcal{A}^i \to \mathcal{B}}, \quad i = 1, 2, \ldots, \\
\left\| \left(\mathcal{R}^1 \right)^\dagger \right\| &:= \left\| \left(\mathcal{R}^1 \right)^\dagger \right\|_{\mathcal{B} \to \mathcal{A}},
\end{aligned} \tag{2.6}$$

for brevity.

Using Proposition 2.1 and the assumption on the left inverse, the main theorem of this paper is given as follows.

Theorem 2.2. *Assume that there exists $(\mathcal{R}^1)\dagger$ such that $(R^1)^\dagger \mathcal{R}^1 = id$ and $\|(\mathcal{R}^1)^\dagger\|$ is bounded, and let*

$$\|\delta x\| \leq \frac{1}{2\|\mathcal{R}\|}. \tag{2.7a}$$

Then,

$$\left\| \delta x^\dagger - \delta x \right\| \leq C^\dagger \|\delta x\|^2, \tag{2.7b}$$

$$\left\| \delta x^B - \delta x \right\| \leq C^B \|\delta x\|^3, \tag{2.7c}$$

where

$$C^\dagger := 2\left\|\left(\mathcal{R}^1\right)^\dagger\right\| \|\mathcal{R}\|^2 \|\Phi\|,$$

$$C^B := \frac{(C^\dagger)^3}{4\|\mathcal{R}\|} + \left(C^\dagger\right)^2 + \|\mathcal{R}\|C^\dagger = C^\dagger\|\mathcal{R}\|\left(\frac{C^\dagger}{2\|\mathcal{R}\|} + 1\right)^2.$$

(2.8)

Proof. By (1.3) and (1.6), we obtain

$$\mathcal{R}^1\left(\delta x^\dagger - \delta x\right) = \mathcal{R}^2(\delta x)^2 + \mathcal{R}^3(\delta x)^3 + \cdots.$$

(2.9)

Therefore we arrive at (2.7b) by the following inequality:

$$\left\|\delta x^\dagger - \delta x\right\| \le \left\|\left(\mathcal{R}^1\right)^\dagger\right\|\frac{(\|\mathcal{R}\|\|\delta x\|)^2\|\Phi\|}{1 - (\|\mathcal{R}\|\|\delta x\|)} \le C^\dagger\|\delta x\|^2.$$

(2.10)

From (2.7a) and (2.7b), we obtain the following upper bound of $\|\delta x^\dagger\|$:

$$\left\|\delta x^\dagger\right\| \le \left(1 + C^\dagger\|\delta x\|\right)\|\delta x\| \le \left(1 + \left\|\left(\mathcal{R}^1\right)^\dagger\right\|\|\mathcal{R}\|\|\Phi\|\right)\|\delta x\|.$$

(2.11)

Using (2.2) and (2.9), we obtain

$$\mathcal{R}^1\left(\delta x - \delta x^B\right) = \mathcal{R}^2(\delta x)^2 - \mathcal{R}^2\left(\delta x^\dagger\right)^2 + \mathcal{R}^3(\delta x)^3 + \mathcal{R}^4(\delta x)^4 + \cdots.$$

(2.12)

The second-order term on the righthand side of (2.12) is analyzed as follows:

$$\mathcal{R}^2(\delta x)^2 - \mathcal{R}^2\left(\delta x^\dagger\right)^2 = \mathcal{R}(\delta x, \mathcal{R}(\delta x, \Phi)) - \mathcal{R}\left(\delta x^\dagger, \mathcal{R}\left(\delta x^\dagger, \Phi\right)\right)$$
$$= \mathcal{R}\left(\delta x, \mathcal{R}\left(\delta x - \delta x^\dagger, \Phi\right)\right) + \mathcal{R}\left(\delta x - \delta x^\dagger, \mathcal{R}\left(\delta x^\dagger, \Phi\right)\right).$$

(2.13)

From (2.12), we obtain

$$\left\|\delta x - \delta x^B\right\| \le \left\|\left(\mathcal{R}^1\right)^\dagger\right\|\left[\left\|\mathcal{R}^2(\delta x)^2 - \mathcal{R}^2\left(\delta x^\dagger\right)^2\right\| + \left\|\mathcal{R}^3(\delta x)^3 + \mathcal{R}^4(\delta x)^4 + \cdots\right\|\right].$$

(2.14)

(I) Compute the solution $\Phi(x)$ and the Robin function $R(x)$ and its first
and second derivatives.
(II) Find $\delta x^\dagger$ by solving $\mathcal{R}^1(\delta x^\dagger) = \Phi(x + \delta x) - \Phi(x)$ as in (1.6).
(III) Find $\delta x^\Delta = \delta x^B - \delta x^\dagger$ by solving $\mathcal{R}^1(\delta x^\Delta) = -\mathcal{R}^2(\delta x^\dagger)$ as in (2.2).
(IV) Compute δx^B by adding $\delta x^\dagger$ and δx^Δ.

Algorithm 1: Numerical algorithm (continuous version).

By using (2.3), (2.10), (2.11), (2.13), and the definition of $C^\dagger$, (2.7c) is achieved from (2.14) as follows:

$$
\begin{aligned}
\left\| \delta x - \delta x^B \right\| &\le \left\| \left(\mathcal{R}^1 \right)^\dagger \right\| \|\Phi\| \left[\|\mathcal{R}\|^2 \left\| \delta x - \delta x^\dagger \right\| \left(\|\delta x\| + \left\| \delta x^\dagger \right\| \right) + \frac{(\|\mathcal{R}\|\|\delta x\|)^3}{1 - \|\mathcal{R}\|\|\delta x\|} \right] \\
&\le \left\| \left(\mathcal{R}^1 \right)^\dagger \right\| \|\Phi\|\|\mathcal{R}\|^2\|\delta x\|^3 \left[C^\dagger \left(2 + \left\| \left(\mathcal{R}^1 \right)^\dagger \right\| \|\mathcal{R}\|\|\Phi\| \right) + 2\|\mathcal{R}\| \right] \\
&\le C^\dagger \|\delta x\|^3 \left[C^\dagger \left(1 + \frac{C^\dagger}{4\|\mathcal{R}\|} \right) + \|\mathcal{R}\| \right] \\
&\le C^B \|\delta x\|^3.
\end{aligned}
\tag{2.15}
$$

$\square$

3. Numerical Algorithm

Assume that we can measure the photon density distribution $\Phi(x+\delta x)$ and $\Phi(x)$ on the entire boundary $\partial\Omega$. That is to say, we have infinite detectors and one source. Then, the numerical algorithm is given as follows.

The detailed computation of the integral operators $\mathcal{R}^1$ and $\mathcal{R}^2$, which is introduced in (1.5), is as follows:

$$
\mathcal{R}^1(\delta x) = \mathcal{R}_{\mu_a}(\delta\mu_a, \Phi) + \mathcal{R}_\kappa(\delta\kappa, \Phi),
\tag{3.1a}
$$

$$
\begin{aligned}
\mathcal{R}^2(\delta x) = {}& \mathcal{R}_{\mu_a}\big(\delta\mu_a, \mathcal{R}_{\mu_a}(\delta\mu_a, \Phi)\big) + \mathcal{R}_{\mu_a}\big(\delta\mu_a, \mathcal{R}_\kappa(\delta\kappa, \Phi)\big), \\
& + \mathcal{R}_\kappa\big(\delta\kappa, \mathcal{R}_{\mu_a}(\delta\mu_a, \Phi)\big) + \mathcal{R}_\kappa\big(\delta\kappa, \mathcal{R}_\kappa(\delta\kappa, \Phi)\big).
\end{aligned}
\tag{3.1b}
$$

3.1. Discretization

Algorithm 1 is based on one source and infinite detectors. However, for practical reasons, we need to discretize Algorithm 1 to obtain the numerical algorithm for finite sources and finite detectors for finite frequencies. The following notations will be used for the discretization:

(i) N_d detector positions: r_{i_d} for $i_d = 1, 2, \ldots, N_d$,

(ii) N_s source functions: $q_{i_s} = \delta_{i_s}$ (Dirac delta function) for $i_s = 1, 2, \cdots, N_s$,

(iii) N_ω frequencies: ω_{i_ω} for $i_\omega = 1, 2, \ldots, N_\omega$,

(iv) N_e elements: T_{i_e} for $i_e = 1, 2, \ldots, N_e$,

(v) N_n nodes: t_{i_n} for $i_n = 1, 2, \ldots, N_n$,

(vi) the measurement index: $j = (i_\omega - 1)N_s N_d + (i_s - 1)N_d + i_d$,

(vii) the optical coefficient index: $k = (i_{\mu\kappa} - 1)N_e + i_e$, where $i_{\mu\kappa}$ is 1 (the absorption coefficient) or 2 (the diffusion coefficient).

If we use piecewise linear or bilinear finite element method, the finite element solution is represented by

$$u_h(x) = \sum_{i_n=1}^{N_n} u_h(i_n)\phi_{i_n}(x), \tag{3.2}$$

where ϕ_{i_n} is the piecewise linear or the bilinear function which is 1 on the i_nth node and 0 on all the other nodes. Assume μ_a and κ are piecewise constant function, which is constant for each N_e finite elements. Therefore, in diffuse optical tomography inverse problem, we have $N_\omega N_s N_d$ measurement information contents and $2N_e$ variables to find.

We should discretize $\mathcal{R}^1$ and $\mathcal{R}^2$ to obtain a discretized version of Algorithm 1. Let the Jacobian and Hessian matrices, which is the discretization of integral operators $\mathcal{R}^1$ and $\mathcal{R}^2$, be J and H. The relation between higher order derivatives for the diffusion operator and higher order terms of Born expansions including $\mathcal{R}^1$ and $\mathcal{R}^2$ is analyzed in [7].

Firstly, let us discretize δx, Φ, and the Robin function R as follows:

$$\delta x \approx \left(\sum_{i_e=1}^{N_e} \delta\mu_{i_e} \chi_{T_{i_e}}, \sum_{i_e=1}^{N_e} \delta\kappa_{i_e} \chi_{T_{i_e}} \right), \tag{3.3a}$$

$$\Phi^{i_\omega, i_s} \approx \sum_{i_n=1}^{N_n} \Phi_{i_n}^{i_\omega, i_s} \phi_{i_n}, \tag{3.3b}$$

$$R^{i_\omega}(\cdot, r_{i_s}) \approx \sum_{i_n=1}^{N_n} R_{i_n}^{i_\omega, i_s} \phi_{i_n}. \tag{3.3c}$$

Since we chose the source function q_s as the Dirac delta function at the i_sth source point, $\Phi^{i_\omega, i_s} = R^{i_\omega}(\cdot, r_{i_s})$. However, we will discriminate these two functions in this paper, since they are different for general source function q which is different from the Dirac delta function. We will use $\delta\mu$ instead of $\delta\mu_a$ for notational convenience.

Let the vector γ_0 which corresponds to the discretization of δx in (3.3a) be defined as

$$\gamma_0 = (\delta\mu_1, \delta\mu_2, \ldots, \delta\mu_{N_e}, \delta\kappa_1, \delta\kappa_2, \ldots, \delta\kappa_{N_e}). \tag{3.4}$$

By the adjoint method [12], $R^{i_\omega}(r_{i_d}, \cdot) = (R^{i_\omega}(\cdot, r_{i_d}))^*$, where * denotes complex conjugate. Likewise for (3.3a), let γ, $\gamma^\dagger$, γ^Δ, and γ^B be the discretization of δx, $\delta x^\dagger$, δx^Δ, and δx^B, respectively.

For a function f and a measurable set T, let us denote $f \in T$ if the intersection of the support of f and T is not empty. The discretization of the linearized solution $\gamma^\dagger$ is attained by solving the following equation:

$$J\gamma^\dagger = b, \tag{3.5}$$

where

$$J(j,k) = \sum_{\phi_{i_{n1}} \in T_{i_e}} \sum_{\phi_{i_{n2}} \in T_{i_e}} \left(R_{i_{n1}}^{i_\omega, i_d}\right)^* E_{i_e}(i_{n1}, i_{n2}) \Phi_{i_{n2}}^{i_\omega, i_s} \quad \text{when } i_{\mu\kappa} = 1,$$

$$J(j,k) = \sum_{\phi_{i_{n1}} \in T_{i_e}} \sum_{\phi_{i_{n2}} \in T_{i_e}} -3\left(R_{i_{n1}}^{i_\omega, i_d}\right)^* \kappa_{i_e}^2 F_{i_e}(i_{n1}, i_{n2}) \Phi_{i_{n2}}^{i_\omega, i_s} \quad \text{when } i_{\mu\kappa} = 2,$$

$$b(j) = \Phi^{i_\omega, i_s}(x + \delta x)(r_{i_d}) - \Phi^{i_\omega, i_s}(x)(r_{i_d}), \tag{3.6}$$

$$E_{i_e}(i_{n1}, i_{n2}) = \int_{T_{i_e}} \phi_{i_{n1}}(\xi) \phi_{i_{n2}}(\xi) d\xi,$$

$$F_{i_e}(i_{n1}, i_{n2}) = \int_{T_{i_e}} \nabla \phi_{i_{n1}}(\xi) \cdot \nabla \phi_{i_{n2}}(\xi) d\xi.$$

The discretized solution γ^Δ is obtained by solving the following equation:

$$J\gamma^\Delta = \left(\gamma^\dagger\right)^t H \gamma^\dagger, \tag{3.7}$$

where

$$H(j, i_{e1}, i_{e2}) = \sum_{\phi_{i_{n1}} \in T_{i_{e1}}} \sum_{\phi_{i_{n2}} \in T_{i_{e2}}} \left(R_{i_{n1}}^{i_\omega, i_d}\right)^* (H_{\mu\mu} + H_{\mu\kappa} + H_{\kappa\mu} + H_{\kappa\kappa})(i_{e1}, i_{e2}; i_{n1}, i_{n2}) \Phi_{i_{n2}}^{i_\omega, i_s}, \tag{3.8}$$

where $H_{\mu\mu}$, $H_{\mu\kappa}$, $H_{\kappa\mu}$, and $H_{\kappa\kappa}$ are the discretization of corresponding terms in (3.1b) such that

$$H_{\mu\mu}(i_{e1}, i_{e2}; i_{n1}, i_{n2}) = \int_{T_{i_{e1}}} \int_{T_{i_{e2}}} \phi_{i_{n1}}(\xi) R^{i_\omega}(\xi, \eta) \phi_{i_{n2}}(\eta) d\xi d\eta,$$

$$H_{\mu\kappa}(i_{e1}, i_{e2}; i_{n1}, i_{n2}) = \int_{T_{i_{e1}}} \int_{T_{i_{e2}}} \phi_{i_{n1}}(\xi) \nabla_\eta R^{i_\omega}(\xi, \eta) \cdot \nabla_\eta \phi_{i_{n2}}(\eta) d\xi d\eta,$$

$$H_{\kappa\mu}(i_{e1}, i_{e2}; i_{n1}, i_{n2}) = \int_{T_{i_{e1}}} \int_{T_{i_{e2}}} \nabla_\xi \phi_{i_{n1}}(\xi) \cdot \nabla_\xi (R^{i_\omega}(\xi, \eta)) \phi_{i_{n2}}(\eta) d\xi d\eta,$$

$$H_{\kappa\kappa}(i_{e1}, i_{e2}; i_{n1}, i_{n2}) = \int_{T_{i_{e1}}} \int_{T_{i_{e2}}} \nabla_\xi \phi_{i_{n1}}(\xi) \cdot \left[\nabla_\xi \nabla_\eta R^{i_\omega}(\xi, \eta)\right] \nabla_\eta \phi_{i_{n2}}(\eta) d\xi d\eta. \tag{3.9}$$

> (I) Compute the solution $\Phi(\gamma_0)_{i_n}^{i_\omega, i_s}$ and the Robin function $R(\gamma_0)_{i_d, i_n}^{i_\omega}$ for
> $i_\omega = 1, \cdots, N_\omega, i_s = 1, \ldots, N_s, i_n = 1, \ldots, N_n$ as in (3.3b) and (3.3c),
>   respectively.
> (II) Find $\gamma^\dagger$ by solving the equation (3.5).
> (III) Find γ^Δ by solving the equation (3.7).
> (IV) Compute γ^B by adding $\gamma^\dagger$ and γ^Δ.

Algorithm 2: Numerical algorithm (discretized version).

Even though the Hessian is not discretized, we obtain the following discretized numerical algorithm (Algorithm 2), expecting the Hessian is simply discretized and approximated in the next subsection:

3.2. Approximation of Hessian

In this subsection we approximate $H_{\mu\mu}$, by assuming κ and μ'_s are constant in Ω. The approximation is progressed in three ways.

First, we approximate the Robin function $R(\xi, \eta)$ when $(\xi, \eta) \in \Omega \setminus \partial\Omega$ by its leading term $R_0(\xi, \eta)$ defined by

$$
R_0(\xi, \eta) = \begin{cases} \dfrac{1}{(p-2)g_p \kappa(\eta)} |\xi - \eta|^{2-p} & p \geq 3, \\[3mm] \dfrac{1}{\omega_2 \kappa(\eta)} \log\left(\dfrac{2S}{|\xi - \eta|}\right) & p = 2, \end{cases}
\tag{3.10}
$$

where g_p is the hypersurface area of the unit sphere in $\mathbb{R}^p$, $p = 2, 3, \ldots$ and $S = \sup_{\xi, \eta \in \Omega} |\xi - \eta|$. Some important relations between R and R_0 are found in [13].

Second, when $i_{e_1} \neq i_{e_2}$, the Robin function R and ϕ_{i_n} are approximated by constant values $R_0(c(i_{e_1}), c(i_{e_2}))$ and $\phi_{i_n}(c(i_e))$ in T_{i_e}, respectively, where $c(i_e)$ of the center of the element T_{i_e}. That is to say, when $i_{e1} \neq i_{e2}$, (3.9) is approximated as follows:

$$
H_{\mu\mu}(i_{e1}, i_{e2}; i_{n1}, i_{n2}) = R_0(c(i_{e1}), c(i_{e2})) \int_{T_{i_{e1}}} \phi_{i_{n1}}(\xi) d\xi \int_{T_{i_{e2}}} \phi_{i_{n2}}(\eta) d\eta.
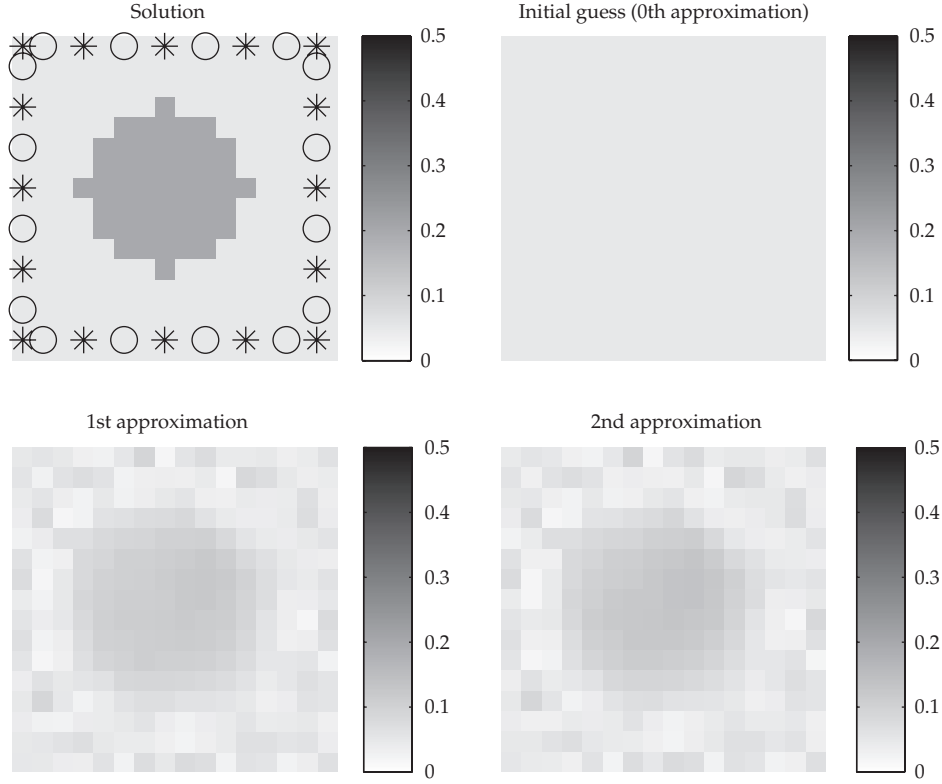\tag{3.11}
$$

Third, when $i_{e1} = i_{e2}$, we use the following lemma.

Lemma 3.1. *Let the measurable set T be contained in $\mathbb{R}^p$, $p = 2, 3, \ldots$, and $0 < m < p$; then, the following inequality holds for T:*

$$
\iint_T |\xi - \eta|^{-m} d\xi\, d\eta \leq \frac{p^{1-m/p}}{p-m} g_p^{m/p} |T|^{2-m/p}, \quad p \geq 2,
\tag{3.12a}
$$

$$
\iint_T \log\left(\frac{2S}{|\xi - \eta|}\right) d\xi\, d\eta \leq \frac{1}{4\pi}\left(1 + \log\left(\frac{4S^2\pi}{|T|}\right)\right) |T|^2, \quad p = 2,
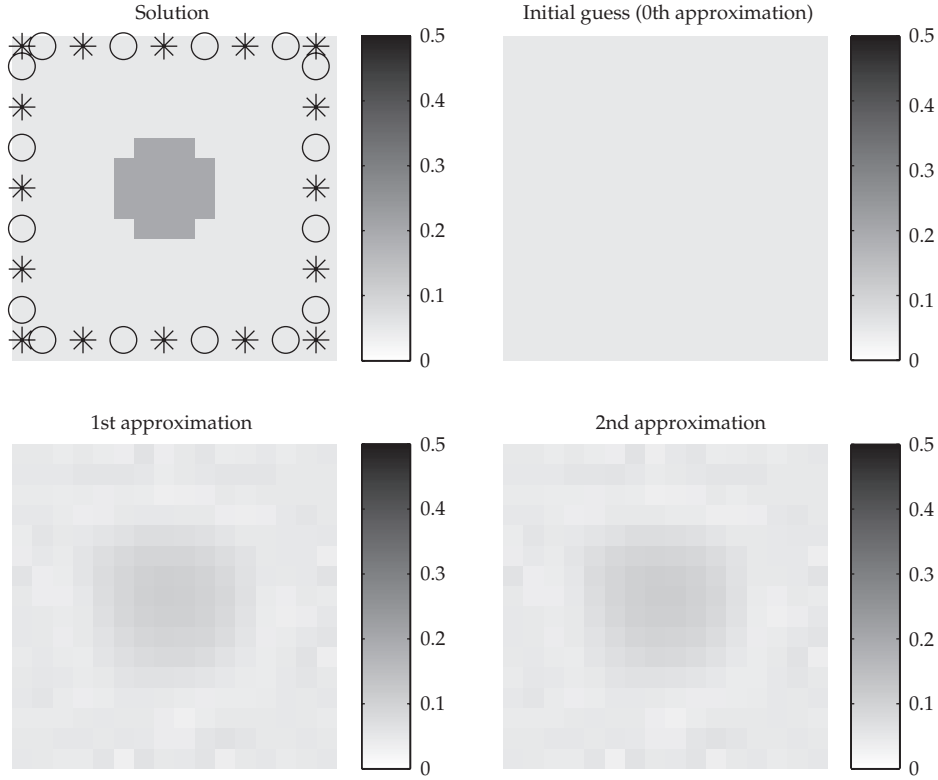\tag{3.12b}
$$

where $|T|$ is the volume of T.

Figure 1: $Jindex = Nx * Ny * 0.4$, $Jalpha = 6.4920e - 009$, 10% noise, sources (∗), and detectors (o).

Proof. If a ball with a radius r has the same volume as T, we have

$$r = \left(|T|\frac{p}{g_p}\right)^{1/p} \tag{3.13}$$

for the space dimensions $p = 2, 3, \ldots$. Let the ball of radius r with center $\xi \in T$ be B_ξ. Let $T_0 = T \cap B_\xi$, $T^+ = T \setminus B_\xi$, and $T^- = B_\xi \setminus T$. Noting that $|T^+| = |T^-|$, we obtain

$$
\begin{aligned}
\int_T |\xi - \eta|^{-m} d\eta &= \int_{T_0} |\xi - \eta|^{-m} d\eta + \int_{T^+} |\xi - \eta|^{-m} d\eta \\
&\leq \int_{T_0} |\xi - \eta|^{-m} d\eta + \int_{T^-} |\xi - \eta|^{-m} d\eta = \int_{B_\xi} |\xi - \eta|^{-m} d\eta \\
&\leq \int_0^r \rho^{p-m-1} g_p d\rho = \frac{g_p}{p-m} r^{p-m} \\
&\leq \frac{g_p}{p-m} \left(|T|\frac{p}{g_p}\right)^{1-m/p}
\end{aligned}
\tag{3.14}
$$

Figure 2: $Jindex = Nx * Ny * 0.4$, $Jalpha = 6.5711e - 009$, 10% noise, sources (∗), and detectors (o).

for all $\xi \in T$. Therefore,

$$\iint_T |\xi - \eta|^{-m} d\eta d\xi \leq \frac{g_p|T|}{p-m}\left(|T|\frac{p}{g_p}\right)^{1-m/p} = \frac{p^{1-m/p}}{p-m} g_p^{m/p} |T|^{2-m/p}. \tag{3.15}$$
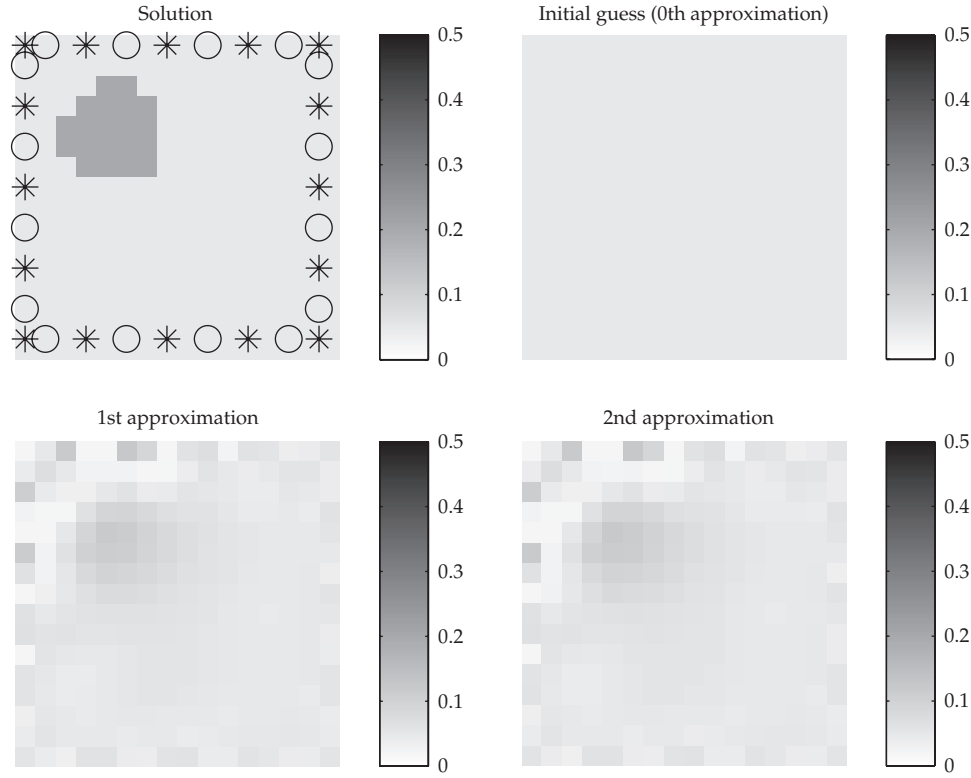
Equation (3.12b) is derived in the same manner. □

Therefore, when $i_{e1} = i_{e2}$, (3.9) is approximated using the inequality in Lemma 3.1 as follows:

$$H_{\mu\mu}(i_{e1}, i_{e1}; i_{n1}, i_{n2}) \approx \phi_{i_{n1}}(c_{i_{e1}})\phi_{i_{n2}}(c_{i_{e1}}) \cdot \begin{cases} \dfrac{p^{2/p}|T_{i_{e1}}|^{1+2/p}}{2(p-2)g_p^{2/p}\kappa(c(i_{e1}))} & p \geq 3, \\[3mm] \dfrac{1}{8\pi^2\kappa(c(i_{e1}))}\left(1 + \log\left(\dfrac{4S^2\pi}{|T_{i_{e1}}|}\right)\right)|T_{i_{e1}}|^2 & p = 2. \end{cases} \tag{3.16}$$

4. Numerical Implementation

In the numerical implementation, the following parameters are used:

Figure 3: $Jindex = Nx * Ny * 0.3$, $Jalpha = 1.8227e - 7$, 10% noise, sources ($*$) and detectors (o).

$\quad$ (i) $\Omega = [0, 6] \times [0, 6]$ (cm^2),

$\quad$ (ii) $N_d = 16$,

$\quad$ (iii) $N_s = 16$,

$\quad$ (iv) $N_\omega = 1$,

$\quad$ (v) $Nx = Ny = 16$,

$\quad$ (vi) $N_e = Nx * Ny$,

$\quad$ (vii) $N_n = (Nx + 1) * (Ny + 1)$,

$\quad$ (viii) $\mu_a = 0.05 + (0.2 - 0.05)\chi_D$ (cm^{-1}),

$\quad$ (ix) $\mu'_s = 8$ (cm^{-1}),

$\quad$ (x) $\kappa = 1/3 * (\mu_a + \mu'_s) = 1/3 * (0.05 + 8)$,

$\quad$ (xi) $\omega = 2\pi * 300$ MHz,

$\quad$ (xii) $a = 1$,

$\quad$ (xiii) $Jindex = Nx * Ny * 0.4$.

$\quad$ Since the diffusion coefficient κ is constant, the right-hand side b is a $N_s * N_d$ column vector, Jacobian J is a $(N_s * N_d) \times N_e$ matrix, the Hessian H is a $N_e \times (Ns * Nd) \times N_e$ third-order tensor, and $(\gamma^\dagger)^t H \gamma^\dagger$ is $Ns * Nd$ column vector in (3.5) and (3.7). $H = H_{\mu\mu}$ is approximated by (3.11) and (3.16).
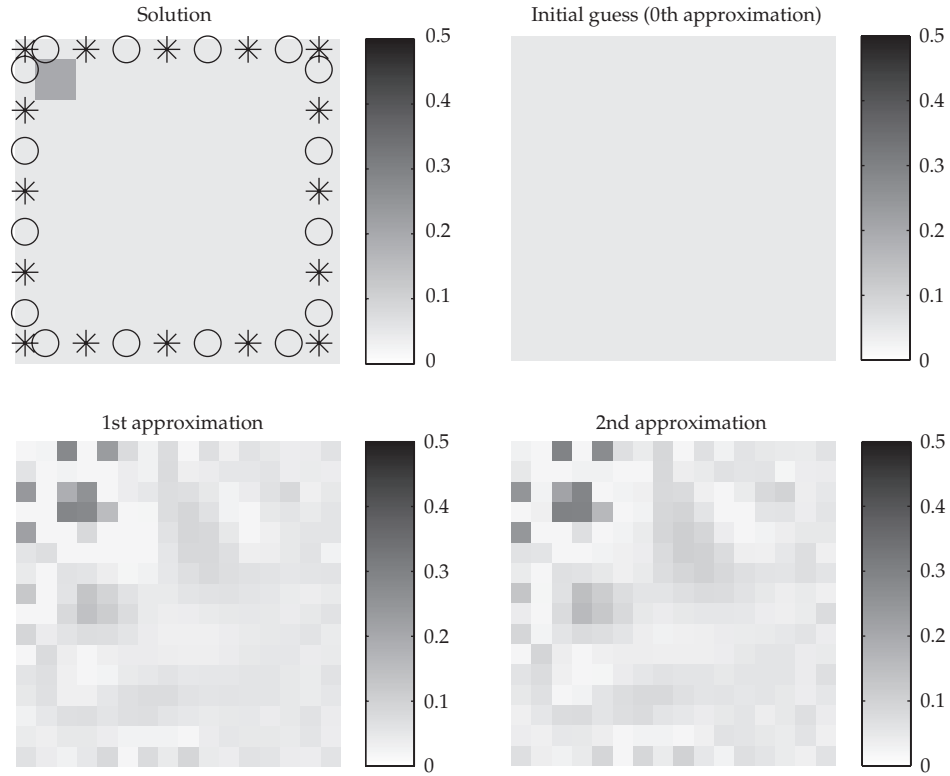
Figure 4: $Jindex = Nx * Ny * 0.4$, $Jalpha = 6.5029e - 009$, 10% noise, sources (∗), and detectors (o).

In the above setting, we reconstruct the obstacle D which has different absorption coefficient ($0.2 \, \text{cm}^{-1}$) compared to the background absorption coefficient ($0.05 \, \text{cm}^{-1}$). Four cases of the obstacle D are considered in Figures 1, 2, 3, and 4. The reconstruction of the absorption coefficient $\mu_a = 0.05 + (0.2 - 0.05)\chi_D$ (cm^{-1}) is implemented using two algorithms. One is the suggested Algorithm 2 based on the second-order Born approximation. The other is linearized method based on the first-order Born approximation, which is equivalent to the step I and II in Algorithm 2. We denoted these two methods in the figures: the 2nd order approximation and the 1st-order approximation, respectively. On the upper-left part of the figures, original μ_a and source/detector locations are plotted. The initial guess (μ_{a0} or γ_0) for the absorption coefficient is plotted on the upper-right part of the figures. In the lowerleft and lowerright part of each figure, reconstructed absorption coefficients by the first approximation ($\mu_a^\dagger$ or $\gamma^\dagger$) and the second approximation (μ_a^B or γ^B) are plotted, respectively.

In all four cases, 10% noise is added. Truncated singular value decomposition(SVD) is used. $Jindex$ is the number of largest singular values used in the truncated SVD method. We used the Tikhonov regularization parameter $Jalpha$ as the value of the $Jindex$th largest singular values.

As is shown in the figure, the discrimination between background and the obstacle is clearer in the second-order approximation than the first-order approximation. The reconstructed image resolution depends on the distance from the boundary of the tissue, which is verified by comparing Figures 1 and 2 with Figures 3 and 4. And the resolution also depends on the size of obstacle, which is verified by comparing Figures 1 and 3 with Figures 2

and 4. Due to the diffusion property of near infrared light, the reconstructed image is much blurred especially in Figure 3. The sensitivity to the noise made some kind of irregular checkerboard pattern near the boundary (Figures 1, 3, and 4).

5. Conclusions

We derived a new numerical method based on the second-order Born approximation. The method is a method of order 3, which is more accurate than the well-known linearized method based on the first-order Born approximation. The error analysis for the method is proved, and the computation of the second-order term is explained using some approximation and integral inequalities. The comparison between the suggested and the linearized method is implemented for four different kinds of absorption coefficients. In the implementation, the suggested method shows more discrimination between the optical obstacle and the background than the linearized method. If more accurate numerical quadrature with more efficient approximation of the Robin function is used, the efficiency of the present method will be elaborated. The simultaneous reconstruction of the absorption and the reduced scattering coefficients based on the proper approximation on the second derivatives of the Robin function would be an interesting topic.

Acknowledgment

References

[1] S. R. Arridge and J. C. Schotland, "Optical tomography: forward and inverse problems," *Inverse Problems*, vol. 25, pp. 1–59, 2009.

[2] V. Isakov, "On uniqueness in the inverse transmission scattering problem," *Communications in Partial Differential Equations*, vol. 15, no. 11, pp. 1565–1587, 1990.

[3] K. Kwon, "Identification of anisotropic anomalous region in inverse problems," *Inverse Problems*, vol. 20, no. 4, pp. 1117–1136, 2004.

[4] K. Kwon and D. Sheen, "Anisotropic inverse conductivity and scattering problems," *Inverse Problems*, vol. 18, no. 3, pp. 745–756, 2002.

[5] J. Sylvester and G. Uhlmann, "A global uniqueness theorem for an inverse boundary value problem," *Annals of Mathematics*, vol. 125, no. 1, pp. 153–169, 1987.

[6] H. Kang, K. Kwon, and K. Yun, "Recovery of an inhomogeneity in an elliptic equation," *Inverse Problems*, vol. 17, no. 1, pp. 25–44, 2001.

[7] K. Kwon and B. Yazıcı, "Born expansion and Fréchet derivatives in nonlinear diffuse optical tomography," *Computers & Mathematics with Applications*, vol. 59, no. 11, pp. 3377–3397, 2010.

[8] V. A. Markel and J. C. Schotland, "Inverse problem in optical diffusion tomography. I. Fourier-Laplace inversion formulas," *Journal of the Optical Society of America A*, vol. 18, no. 6, pp. 1336–1347, 2001.

[9] G. Murat, K. Kwon, B. Yazici, E. Giladi, and X. Intes, "Effect of discretization error and adaptive mesh generation in diffuse optical absorption imaging: I," *Inverse Problems*, vol. 23, no. 3, pp. 1115–1133, 2007.

[10] G. Murat, K. Kwon, B. Yazici, E. Giladi, and X. Intes, "Effect of discretization error and adaptive mesh generation in diffuse optical absorption imaging. II," *Inverse Problems*, vol. 23, no. 3, pp. 1135–1160, 2007.

[11] K. Kwon, B. Yazıcı, and M. Guven, "Two-level domain decomposition methods for diffuse optical tomography," *Inverse Problems*, vol. 22, no. 5, pp. 1533–1559, 2006.

[12] S. R. Arridge, "Optical tomography in medical imaging," *Inverse Problems*, vol. 15, no. 2, pp. R41–R93, 1999.

[13] C. Miranda, *Partial Differential Equations of Elliptic Type*, Springer, New York, NY, USA, 1970.